AIDIC *Conference Series*, Vol. 9, 2009
Editor Sauro Pierucci
DOI: 10.3303/ACOS0909007

ISBN 978-88-95608-10-5 ISSN 2036-5969

SINGLE BUBBLE AND DROP MOTION MODELING

G. Bozzano, M. Dente

Politecnico di Milano, CMIC Department, Italy

A model for the prediction of the terminal relative velocity of single gas bubbles or drops, moving freely into a quiescent phase under gravity, is presented. It is based on the calculation of the shape assumed by the particle during its motion and on its effects on the drag coefficient. Also the influence of contamination is taken into account. The results have been compared with a large set of experimental literature data covering a wide range of physical properties and particle sizes. The agreements are quite satisfactory and confirm the reliability of the model.

1. INTRODUCTION

The characterisation of bubbles or drops motion is essential for many gas-liquid and liquid-liquid operations, not only related to chemical processes but also, for instance, to metallurgy, biotechnology and oceanography. Even if in practical applications they seldom occur in isolation and motion regards swarms, the behavior of the single fluid particle can support a better knowledge of the overall. Modeling the single particle behavior can be considered a quite complex problem by itself, particularly if the purpose is to cover a wide range of properties. Theories and experimental data have been presented along the years, covering different fluid-dynamic regimes, shapes and, correspondingly, drag coefficients (Peebles nad Garber, 1953, Harmathy, 1960; Levich, 1962; Kupferberg and Jameson 1969, Batchelor, 1970; Grace *et al.* 1976, Bhaga and Weber, 1981; Karamanev, 1994, Tomiyama 1998, Nguyen, 1998; Tomiyama *et al.*, 2002, Di Marco *et al.*, 2003, Kelbaliyev *et al.*, 2007 among the others). In all these works two immiscible fluids have been made in contact in adiabatic conditions. Starting from the studies of Hadamard (1911) and Rybczynsky (1911) based on spherical shape fluid particles in completely viscous flow, many studies were performed taking into account different shapes and trying to deduce more or less empirical correlations for the drag coefficient. More detail on these studies is given in Bozzano and Dente (2001), where is proposed a solution for the prediction of shape and velocity of bubbles inside quiescent liquids. Here an extension to the case of drops is presented. The differences are mainly related to the viscosity of the fluid particle. The particle shape is deduced by minimizing the total energy associated to motion.

2. SHAPE OF THE DISPERSED FLUID PARTICLE, DRAG COEFFICIENT AND VELOCITY

It is well known that in fluid particles with sufficiently small diameter (less than about 1 mm) the internal pressure produced by the interfacial tension is sufficiently high to keep them quite spherical. For larger dimensions they become oblate spheroids, and it is also observed an oscillatory way of rise. Moreover there is also a range of critical radius above which the circulations inside the particle become important (Garner and Haycock 1959). This critical radius is obviously also depending on the viscosity of the dispersed phase. Also interfacial contamination deeply affects particle internal circulations.
Levich (1964) and Gaudin (1957) compared the behavior of a bubble rising in liquid with that of a free falling heavy particle following the idea that the forces acting over the particle are the same. This was proved to be incorrect since for high Reynolds number (more than 130) the friction factor tends to a constant value of 0.9 following Bozzano and Dente (1991) and 0.95 following Karamanev and Nikolov (1992), i.e. more than twice the value predicted by Newton law.

Please cite this article as: Bozzano G. and Dente M., (2009), Single bubble and drop motion modeling, AIDIC Conference Series, 09, 53-60 DOI: 10.3303/ACOS0909007

In this work the prevailing motion of the particle is assumed to be linear (secondary motions, i.e. helicoidal, zig-zag, oscillating etc. are neglected). Thanks to the mobility of the interface, as said before a fluid particle behaves differently from that of a rigid body mainly for two aspects: the possibility of modifying the shape and the presence of internal circulations. The last ones strongly affects the resistance offered to the particle motion and the possible development of the boundary layer around the particle.

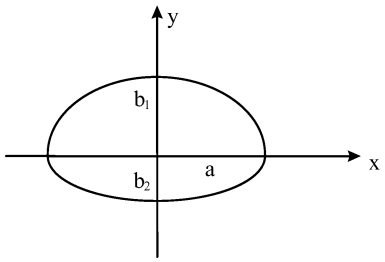

Fig. 1 – Assumed shape of the fluid particle (a, b_1, b_2 = particle major and minor semi-axes)

In the steady state the forces balance gives:

$$\Delta\rho \cdot g \cdot V_p = \pi a^2 \frac{\rho_c U^2}{2} \cdot f \tag{1}$$

From equation 1) the terminal velocity (U) is therefore deduced as a function of the drag coefficient $C_D = \left(\frac{2a}{D_0}\right)^2 \cdot f = Def \cdot f$:

$$U = \left(\frac{4}{3}\frac{\Delta\rho \cdot g \cdot D_0}{\rho_c C_D}\right)^{1/2} \tag{2}$$

The key variable in defining drop motion velocity becomes consequently the drag coefficient C_D. It shows a simple dependence on the friction factor "f" and on the deformation. During the motion the particle assumes the shape that minimizes its total energy. Substantially the energies mainly involved (interfacial, potential and kinetic, already described in Bozzano and Dente, 2001) reflect the influence of interfacial tension, density difference, viscosity and velocity on the particle shape. Contaminants or hydrates (present for instance in the case of methane bubbles or CO_2 drops rising or falling in the deep ocean) at the interface affect its rigidity and the limiting internal circulations. The mapping of the total energy as a function of the particle geometrical properties allows, through its minimization, to deduce the deformation factor "Def" A convenient processing of the shapes obtained by means of the minimization procedure, giving an explicit expression for "Def", has been performed. It allows a direct evaluation of "Def" as a function of Morton and Eotvos numbers, and, therefore, of the physical properties and of the size of the particle:

$$\mathrm{Def} = \left(\frac{2a}{D_0}\right)^2 = \frac{10 \cdot \left(1 + 1.3 \cdot Mo^{1/6}\right) + 3.1 \cdot Eo}{10 \cdot \left(1 + 1.3 \cdot Mo^{1/6}\right) + Eo} \tag{3}$$

The friction factor has been obtained by combination of two asymptotic behaviors, viscous flow: f_{visc} , and Newton's-law flow: f_∞:

$$\mathrm{f}\left(\mathrm{Re}, \mathrm{Eo}\right) = \mathrm{f}_{\mathrm{visc}}\left(\mathrm{Re}, \mathrm{Mo}\right) + \mathrm{f}_{\infty}\left(\mathrm{Eo}, \mathrm{Mo}\right) \tag{4}$$

For spherical shape particles (Def = 1), and low Re values (about above 20 that is usually the case), the drag coefficient has been originally evaluated by Levich (1949) and reviewed by Batchelor (1970) by assuming that

the rate at which buoyancy forces on the particle do work, i.e. UF (where F=drag force), must be equal to the total rate of dissipation in the surrounding fluid:

$$C_D = f_{visc} = \frac{48}{\mathrm{Re}} \tag{5}$$

A correction was proposed by Moore (1963), taking into account also the dissipation in the boundary layer at the particle surface and in the wake:

$$f_{visc} = \frac{48}{\mathrm{Re}}\left(1 - \frac{2.2}{\mathrm{Re}^{1/2}}\right) \tag{6}$$

Because in the expression 6) the negative factor can give place to problems at low Re values, a more satisfactory expression is here proposed:

$$f_{visc} = \frac{48}{\mathrm{Re}} \cdot \frac{\sqrt{1+0.25\,\mathrm{Re}}}{\sqrt{1+0.25\,\mathrm{Re}}+1} \tag{7}$$

Of course, also inside the particles a motion may occur and this internal circulations may affect the flow. No relative movement of the two fluids at the interface can occur and the tangential stress exerted at the interface by the external fluid must be equal and opposite to that exerted by the internal one (Batchelor, 1970). In this way the friction factor results affected by the viscosity ratio of the continuous and dispersed fluids:

$$f_{visc} = \frac{48}{\mathrm{Re}} \cdot \frac{\sqrt{1+0.25\,\mathrm{Re}}}{\sqrt{1+0.25\,\mathrm{Re}}+1} \cdot \frac{3/2+\mu_c/\mu_d}{1+\mu_c/\mu_d} \tag{8}$$

Both the cases of drop ($\mu_c/\mu_d << 1$) and bubbles ($\mu_c/\mu_d >> 1$) are covered by expression 8).

Finally, an other contribution to expression 8) allows to take into account that in high viscosity medium, i.e. for high Mo numbers, the factor “48” is reduced to “16”. The resulting final expression of f_{visc} is:

$$f_{visc} = \frac{48}{\mathrm{Re}} \cdot \frac{\sqrt{1+0.25\,\mathrm{Re}}}{\sqrt{1+0.25\,\mathrm{Re}}+1} \cdot \frac{3/2+\mu_c/\mu_d}{1+\mu_c/\mu_d} \cdot \frac{1+12\cdot Mo^{1/3}}{1+36\cdot Mo^{1/3}} \tag{9}$$

The friction factor for sufficiently high Reynolds numbers (at least 10^4), becomes a constant corresponding to a value of the drag coefficient of about 3 because of the large deformation (quasi-spherical cap shape). The asymptotic friction factor for high Reynolds numbers is also in this case deduced as function of Eo and Mo (by interpolation of the results obtained from the minimization procedure):

$$f_\infty = \frac{C_D\big|_\infty}{DEF\big|_\infty} = 0.9\frac{Eo^{3/2}}{1.4\cdot\left(1+30Mo^{1/6}\right)+Eo^{3/2}} \tag{10}$$

The combined expression of the friction factor, covering all Re numbers, becomes (with c,d = indexes for continuous and dispersed phase):

$$f = \frac{48}{\mathrm{Re}} \cdot \frac{\sqrt{1+0.25\mathrm{Re}}}{\sqrt{1+0.25\mathrm{Re}}+1} \cdot \frac{3/2+\mu_c/\mu_d}{1+\mu_c/\mu_d} \cdot \frac{1+12\cdot Mo^{1/3}}{1+36\cdot Mo^{1/3}} + 0.9\frac{Eo^{3/2}}{1.4\cdot\left(1+30Mo^{1/6}\right)+Eo^{3/2}} \tag{11}$$

Internal circulations of drops are less intensive than inside bubbles, due to the higher viscosity, forcing the detachment of the boundary layer on a larger surface behind and retarding the transition to turbulence.

Therefore, *for drop motion,* the friction factor is modified in:

$$\begin{aligned} &for\ \ f_\infty < 0.45 \quad f = \frac{48}{\mathrm{Re}} \cdot \frac{\sqrt{1+0.25\mathrm{Re}}}{\sqrt{1+0.25\mathrm{Re}}+1} \cdot \frac{3/2+\mu_c/\mu_d}{1+\mu_c/\mu_d} \cdot \frac{1+12\cdot Mo^{1/3}}{1+36\cdot Mo^{1/3}} + 0.45 \\ &for\ \ f_\infty \geq 0.45 \quad f = \frac{48}{\mathrm{Re}} \cdot \frac{\sqrt{1+0.25\mathrm{Re}}}{\sqrt{1+0.25\mathrm{Re}}+1} \cdot \frac{3/2+\mu_c/\mu_d}{1+\mu_c/\mu_d} \cdot \frac{1+12\cdot Mo^{1/3}}{1+36\cdot Mo^{1/3}} + 0.9\frac{Eo^{3/2}}{1.4\cdot\left(1+30Mo^{1/6}\right)+Eo^{3/2}} \end{aligned} \tag{12}$$

This latter expression is valid also in the case of contaminated bubbles. In facts in this situation bubbles have a drag coefficient close to that of a "rigid body" and therefore internal circulations have no detectable influence on the dynamics of the bubble motion.

3. RESULTS AND COMPARISONS

The model has been compared with gas-liquid systems and immiscible liquid-liquid systems. The figures show the agreements among model results (lines), and experimental data (points). They are a representative sample of the total results. Figgs 2-8 refer to air-liquid systems (2 to 6, experiment from Peebles and Garber (1953), Fig. 7 and 8 to those of Haberman and Morton (1956)). Fig. 9 is related to drops of water raining into air (experimental data are taken from E. Loth (2008)). In all the reported comparisons the agreement among model results and experimental data is quite good.

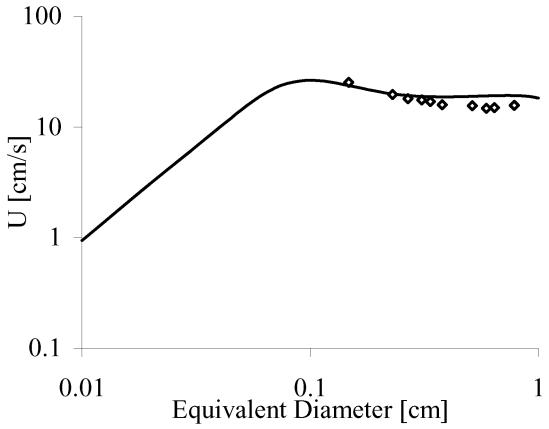

Fig. 2: Air bubbles in ethylacetate

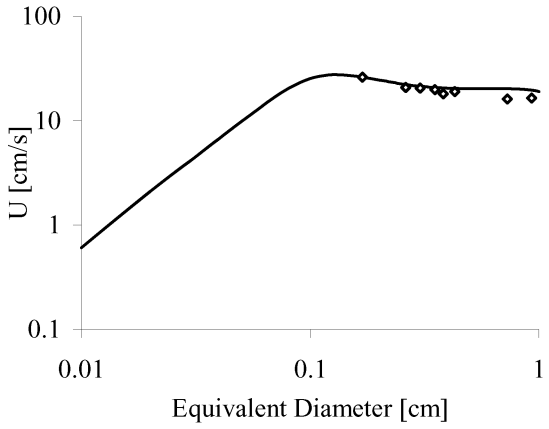

Fig. 3: Air bubbles in pyridine

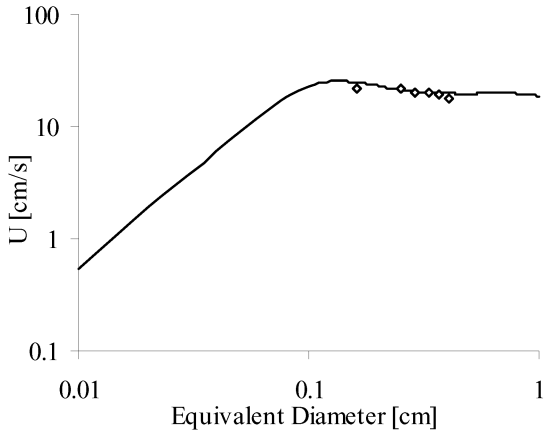

Fig. 4: Air bubbles in 70% Acetic acid –water solution

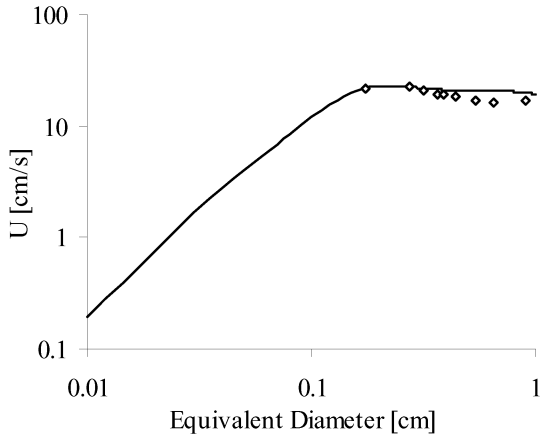

Fig.5: Air bubbles in Aniline

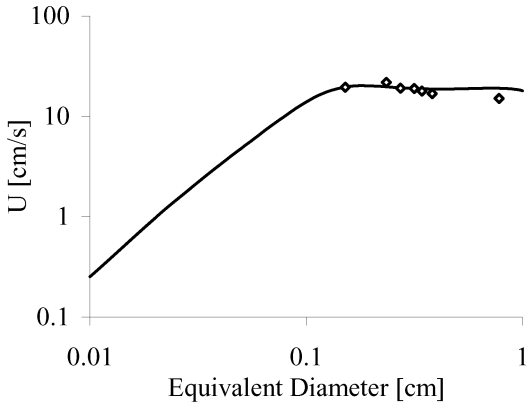

Fig.6: Air bubbles in Isopropyl Alcohol (IPA)

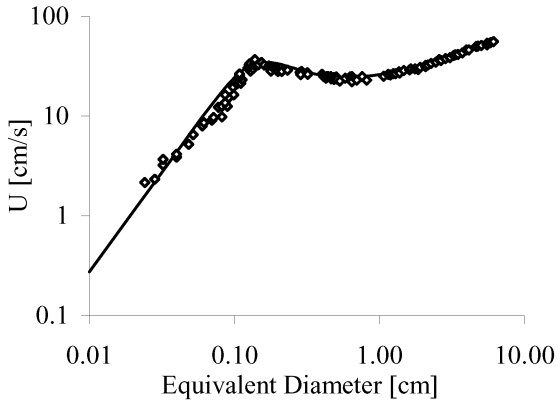

Fig.7: Air bubbles in purified water

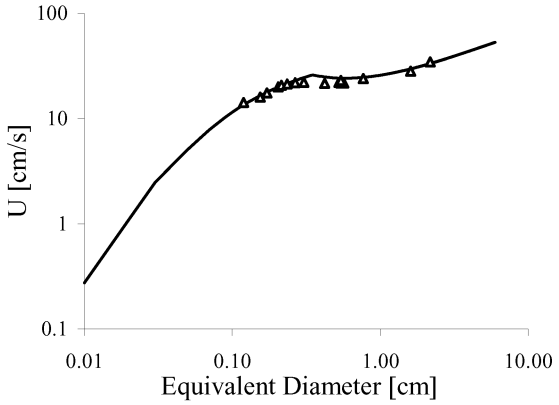

Fig.8: Air bubbles in tap water

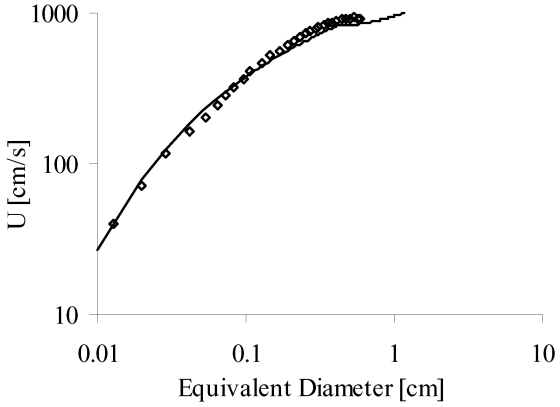

Fig. 9: Drops of rain into air

Table 1: properties of bubbles systems

	AAW	Aniline	IPA	Ethylacetate	Pyridine
ρ_c (g/cm^3)	1.0684	1.02	0.793	0.894	0.987
μ_c (g/cm/s)	0.0104	0.0293	0.0178	0.0047	0.0085
σ (g/s^2)	34.3	41.7	20.7	22.6	36.6

The properties of liquids are reported in Table 1. As is it possible to observe, the data cover a wide range of densities and viscosities of the continuous phase.

Figs 9-14 show liquid-liquid behaviour. Figure 9 reports some interesting data related to the fall of liquid CO_2 drops in the deep Ocean. The experiments (data from Ozaki *et al.*(2001)) where performed at 200 atm and 5°C in order to study the possible CO_2 ocean sequestration by moving ships. A specific paper will be prepared on this e Figs 10-14 compare the model with the data of Shengen Hu and Kintner (1955) on different organic liquids. Table 2 refers to the physical properties of the dispersed and of the continous phase. Also in this case the data cover a wide range of densities and viscosities of the phases.

4. CONCLUSIONS

All the comparisons show the reliability of the proposed model in a wide range of conditions (both for particle size and physical properties). The new approach allows a unified model for the description of bubbles or drops motion into quiescent liquid.

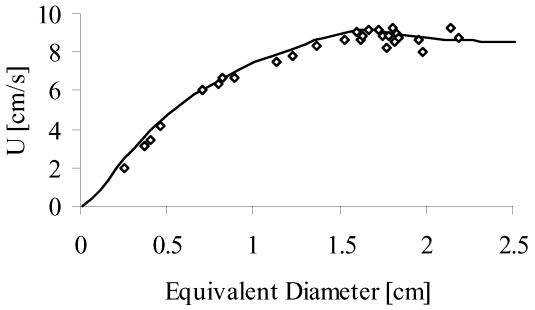

Fig.10: CO_2 drops in deep sea (SW-CO_2)

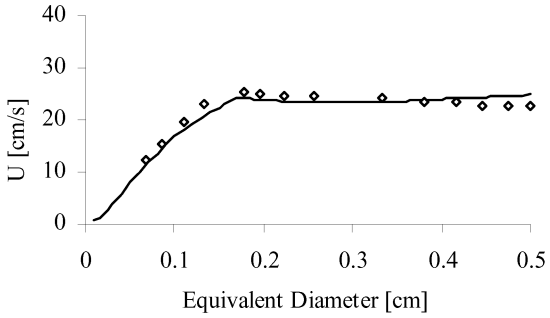

Fig. 11: Water-tetrabromoethane (WT)

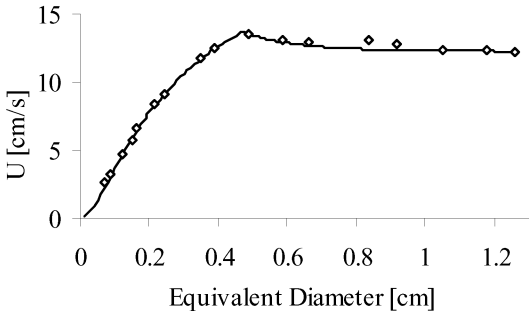

Fig. 12: Water-nitrobenzene (WN).

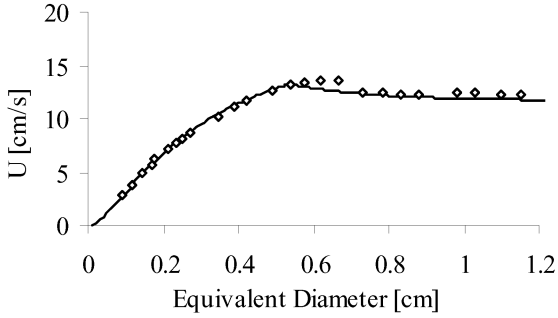

Fig. 13: Water-O-nitrotoluene (WON)

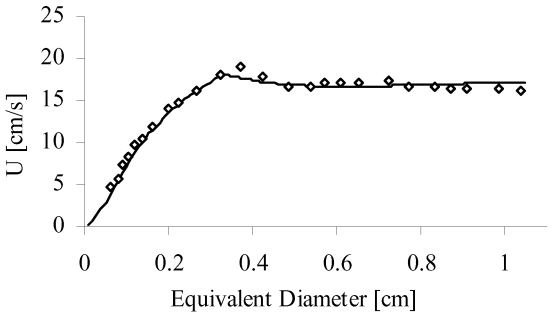

Fig. 14: Water-bromobenzene (WBB)

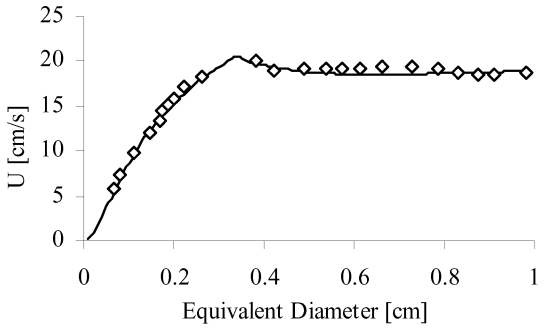

Fig. 15: Water-tetrachloroethylene (WTClE)

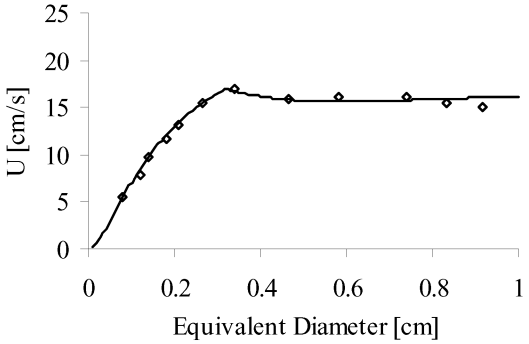

Fig. 16: Water-Ethylbromide (WEB)

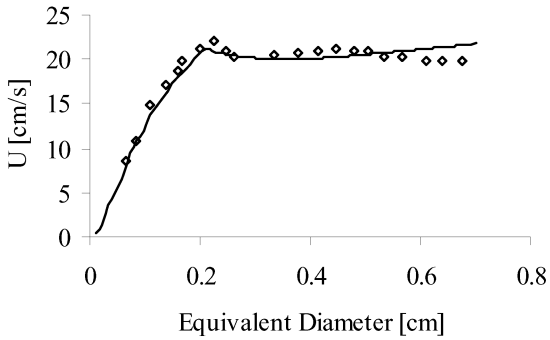

Fig. 17: Water-Dibromoethane (WDBE)

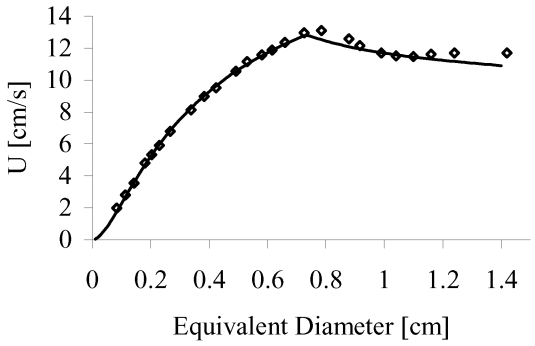

Fig. 17: Water-Clorobenzene (WClB)

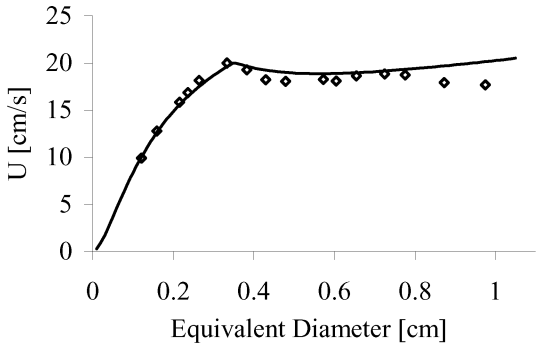

Fig. 18:Water-Carbontetrachloride (WCTC)

Table 2: properties of drop systems (liquid-liquid and gas-liquid)

	$SW-CO_2$	WT	WN	WON	WBB	WTClE
ρ_d (g/cm^3)	1.050	2.9474	1.1947	1.1576	1.4881	1.6143
ρ_c (g/cm^3)	1.024	0.9973	0.9972	0.997	0.9971	0.997
μ_c (g/cm/s)	0.0158	0.008968	0.008835	0.008996	0.008953	0.008946
μ_d (g/cm/s)	0.00125	0.092888	0.017379	0.02036	0.010719	0.008903
σ (g/s^2)	42.0	35.9	28.9	31.3	36.3	44.4
	WEB	WDBE	WClB	WCTC	Drop of rain	
ρ_d (g/cm^3)	1.4478	2.1541	1.0995	1.577	1.0	
ρ_c (g/cm^3)	0.9977	0.9966	0.9969	0.9957	0.0016	
μ_c (g/cm/s)	0.008814	0.008968	0.009036	0.007797	182.7e-6	
μ_d (g/cm/s)	0.004908	0.01582	0.007606	0.008702	0.01	
σ (g/s^2)	30.0	31.9	39.2	45.9	72.9	

5. NOMENCLATURE

D_0 = diameter of the equivalent spherical fluid particle (m)
g = acceleration due to gravity (m/s^2)
ρ = density (kg/m^3)
$\Delta\rho$ = absolute density difference among the phases (kg/m^3)
σ = interfacial tension (N/m)
μ = viscosity (kg/(ms))

Reynolds number: $\mathrm{Re} = \dfrac{\rho_c D_0 U}{\mu_c}$

Eötvös number: $\mathrm{Eo} = \dfrac{\Delta\rho\, g\, D_0^2}{\sigma}$

Morton number: $\mathrm{Mo} = \dfrac{\Delta\rho \cdot g\, \mu_c^4}{\rho_c^2 \sigma^3}$

Subscrits:
c: continuous
d : dispersed

6. REFERENCES

Batchelor, G.K., 1970, *An Introduction to Fluid-dynamics*. Cambridge University Press

Bhaga D. and Weber M.E., 1981, *Bubbles in viscous liquids: shapes, wakes and velocities*, Journal of fluid Mechanics, 105, 61-85

Bozzano G. and Dente M. , 2001, *Shape and terminal velocity of single bubble motion: a novel approach*, Comp. & Chem. Engng., 25, 571-576

Bryn, T., 1949, *David Taylor Model Basin Transl.*, Rep. No 132

Calderbank, P. H., Johnson, D. S. L. and Loudon, J., 1970, *Mechanics and mass transfer of single bubbles in free rise through some newtonian and non-newtonian liquids*, Chem. Eng. Sci., 25, 235-256

Davies R.M. and Taylor F.R.S. Sir Geoffey, 1950, *The mechanics of rising bubbles*, Proceedings of the Royal Society, A200, 375-390

Di Marco, P., Grassi, W. and Memoli, G., 2003. *Experimental study on rising velocity of nitrogen bubbles in FC-72. Int. J. Therm. Sci.* **42**, pp. 435–446

Garner, F. H. , and Haycock, P. I. , *Circulation in Liquid Drops*, Proc. Roy Soc., A., **252**, 457-475 (1959).

Gaudin, A.M. *Flotation*, 2nd ed., McGraw-Hill, New York (1957)

Grace, J.R., Wairegi, T. and Nguyen, T.H., 1976. *Shapes and velocities of single drops and bubbles moving freely through immiscible liquids. Trans. IChemE* **54**, p. 167

Haberman, W. L. and Morton, R. K., 1956, *An experimental study of bubbles moving into liquids*, Soc. Civil Eng. Trans., 121, 227-251

Hadamard, J., 1911, *Movement permanent lent d'une sphere liquide et visqueuse. dans un liquide visqueux*, Comptes Rendus Hebdomadaires des Seances de l' Academie des Sciences, 152, 1735-1743

Harmathy T.Z., 1960, *Velocity of large drops and bubbles in media of infinite or restricted extent*, A.I.Ch.E. Journal, 6, No.2, June, 281-288

Karamanev D.G. , 1994, *Rise of Gas Bubbles in Quiescent Liquids*, A.I.Ch.E. Journal, 40, no. 8, August, 1418-1421

Kupferberg, A. and Jameson, G.J., 1969. *Bubble formation at submerged orifice above a gas chamber of finite volume. Trans. IChemE* **47**, pp. 241–250.

Levich, V.G. , 1962, *Physico-chemical hydrodynamics*, New York, Prentice-Hall

Levich, V.G., 1949, *The motion of bubbles at high Reynolds numbers*, Zh. Eksperim. & Teor. Fiz. 19, 18

Loth, E., 2008, *Quasi-steady shape and drag of deformable bubbles and drops*. International Journal of Multiphase Flow , 34, 523-546

Moore, D.W. , 1963, *The boundary layer on a spherical gas bubble*, J. Fluid Mech., 16, 161-176

Ozaki M. Minamiura J., Kitajima Y., Mizokami S., Takeuchi K. and Hatakenaka K., 2001, *CO_2 ocean sequestration by moving ships*, J. Mar. Sci Technol, 6, 51–58

Peebles, F. N., Garber, H. J., 1953, *Studies on the motion of gas bubbles and liquids*, Chem. Eng. Progr., 49, 88-97

Rybczynski, 1911, *Über die fortschreitende Bewegung einer flüssigen Kugel in einem sachen Medium*, Bull. Intern. Acad. Sci. Cracovie (Ser. A) 1, 40-46.

Shengen Hu, Kintner R.C., 1955, *The fall of single liquid drops through water*, A.I.Ch.E. Journal, 1, No.1, March, 42-48

Tomiyama, A., 1998. *Struggle with computational bubble dynamics*. In: Proceedings of 3rd International Conference on Multiphase Flows (CD-ROM), Lyon, 8–12 June

Tomiyama, A., Celata, G.P., Hosokawa, S. and Yoshida, S., 2002. *Terminal velocity of single bubbles in surface tension force dominant regime*. Int. J. Multiphase Flow **28**, pp. 1497–1519.